Limited temperature response to the very large AD 1258 volcanic eruption

Claudia Timmreck,[1] Stephan J. Lorenz,[1] Thomas J. Crowley,[2] Stefan Kinne,[1] Thomas J. Raddatz,[1] Manu A. Thomas,[1,3] and Johann H. Jungclaus[1]

Received 22 July 2009; revised 8 September 2009; accepted 25 September 2009; published 6 November 2009.

[1] The large AD 1258 eruption had a stratospheric sulfate load approximately ten times greater than the 1991 Pinatubo eruption. Yet surface cooling was not substantially larger than for Pinatubo (~0.4 K). We apply a comprehensive Earth System Model to demonstrate that the size of the aerosol particles needs to be included in simulations, especially to explain the climate response to large eruptions. The temperature response weakens because increased density of particles increases collision rate and therefore aerosol growth. Only aerosol particle sizes substantially larger than observed after the Pinatubo eruption yield temperature changes consistent with terrestrial Northern Hemisphere summer temperature reconstructions. These results challenge an oft-held assumption of volcanic impacts not only with respect to the immediate or longer-term temperature response, but also any ecosystem response, including extinctions.
Citation: Timmreck, C., S. J. Lorenz, T. J. Crowley, S. Kinne, T. J. Raddatz, M. A. Thomas, and J. H. Jungclaus (2009), Limited temperature response to the very large AD 1258 volcanic eruption, *Geophys. Res. Lett.*, *36*, L21708, doi:10.1029/2009GL040083.

1. Introduction

[2] Large eruptions constitute strong forcing to the Earth system by reflecting solar radiation and trapping outgoing longwave radiation. This leads to considerable cooling at the surface and pronounced warming of the stratosphere, thereby substantially altering the atmospheric circulation. A detection and attribution study indicates that volcanism is the most prominent forcing factor for climate variability of the last 700 years [*Hegerl et al.*, 2007].

[3] The largest eruption in the last 7,000 years is the AD 1258 event [*Langway et al.*, 1988], which is manifested by a very large sulfate signal in both Arctic and Antarctic ice cores [*Oppenheimer*, 2003]. Sulfate aerosol transport into both hemispheres suggests a low latitude eruption with an initial injection of 260 ± 60 Tg SO_2 [*Oppenheimer*, 2003]. The location of the eruption is uncertain. One candidate is the eruption of Quilotoa in the Andes (0.5°S, 78.5°W) [*Barberi et al.*, 1995]. The exact timing of the eruption is slightly uncertain. Northern hemisphere tree rings indicate significant cooling in 1258–1259 (Figure S1), but very cold Southern Hemisphere summer temperatures point to a mid 1257 date [*Oppenheimer*, 2003].[4] The total darkening of the eclipsed Moon in May 1258 [*Stothers*, 2000] and peak fallout in Northern Hemisphere winter 1259 suggest an eruption in early 1258 [*Stothers*, 2000]. Historical chronicles report massive rainfall anomalies and severe crop damage and famine across Europe in 1258, but the decadal-scale cooling signal in hemispheric temperature reconstructions of the last millennium is small [*Mann et al.*, 2008].

[4] At present, a physically consistent explanation of the relatively weak temperature response after the 1258 eruption is missing. One reason could be the shift of aerosol size distribution to larger particles due to increased frequency of collisions [*Pinto et al.*, 1989]. Larger particles scatter less visible light and absorb more efficiently in the near- and far-infrared. This conjecture is supported by comparison of the 1258 and Pinatubo eruptions in ice cores. Monthly-scale electrical conductivity measurements of the GRIP and GISP2 ice cores indicate that the lifetime of the 1258 perturbation was virtually the same as for Pinatubo in an Antarctic core (Figure 1a), which in turn tracks observed aerosol optical depth.

[5] Past reconstructions of a volcanic forcing time series over the last millennium contain either no information about particle size distribution [*Crowley*, 2000; *Gao et al.*, 2008] or assume a fixed size distribution [*Ammann et al.*, 2007]. Recently, a new volcanic forcing data set of the last millennium has been compiled [*Crowley et al.*, 2008] (T. J. Crowley et al., An updated millennial reconstruction for mid-high latitude northern hemisphere land areas, manuscript in preparation, 2009), which includes estimates of both aerosol optical depth (AOD) and particle size of stratospheric aerosols. Using this data set, Earth System Model (ESM) simulations are performed to understand the weaker than expected surface cooling after the 1258 eruption. As the suggested particle size estimates are uncertain, sensitivity studies are carried out to examine the climate response as function of aerosol size.

2. Experimental Setup

[6] We utilize the comprehensive ESM developed at the Max Planck Institute for Meteorology (MPI-M) and the new volcanic forcing data set of the last millennium [*Crowley et al.*, 2008]. The full carbon cycle is considered with modules for terrestrial biosphere (JSBACH [*Raddatz et al.*, 2007]) as well as ocean biogeochemistry (HAMOCC5 [*Wetzel et al.*, 2005]). The atmosphere model ECHAM5 [*Roeckner et al.*,

[1]Max-Planck Institute for Meteorology, Hamburg, Germany.
[2]School of GeoSciences, University of Edinburgh, Edinburgh, UK.
[3]Now at School of Environmental Sciences, University of East Anglia, Norwich, UK.

0094-8276/09/2009GL040083$05.00

[4]Auxiliary materials are available in the HTML. doi:10.1029/2009GL040083.

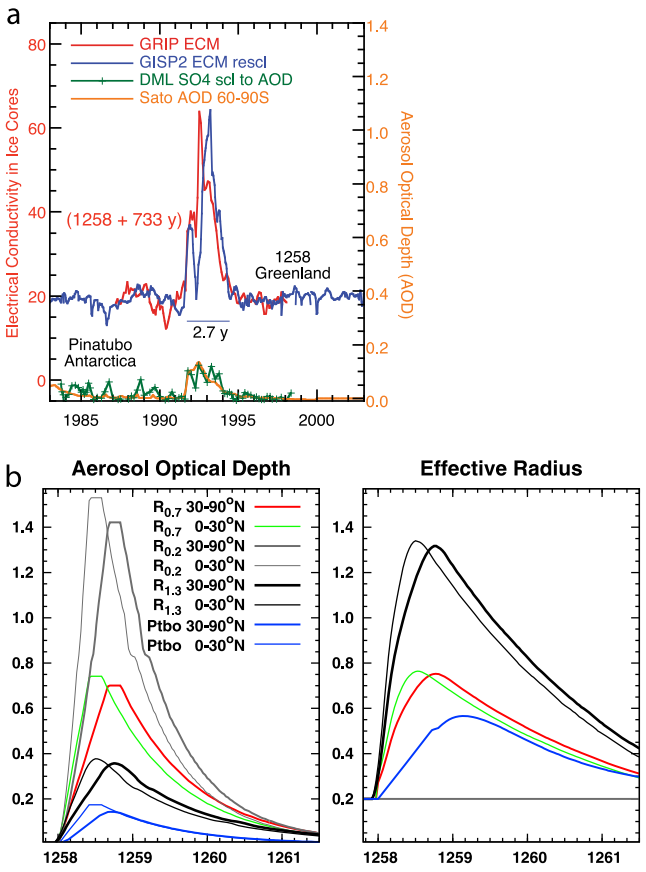

Figure 1. (a) Comparison of electrical conductivity measurements for the GRIP and the GISP2 ice cores [*Clausen et al.*, 1997; *Taylor et al.*, 1997] for the 1258 eruption with Pinatubo life spans estimated from *Sato et al.* [1993] and sub-annual resolution in a Droning Maud Land ice core [*Traufetter et al.*, 2004]. (b) Aerosol Optical Depth (AOD) at 0.55 μm and effective radius for the 1258 volcanic eruption on two of the four latitude bands ($R_{0.7}$, red and green line). Grey lines are same mass as in $R_{0.7}$ but at a constant effective radius ($R_{0.2}$); black lines are same mass as in $R_{0.7}$ but at a higher effective radius ($R_{1.3}$). Also shown are AOD and R_{eff} values (blue lines) for the Pinatubo eruption but at an artificial start date.

2006] is run at T31 resolution (3.75° × 3.75° spatial resolution), with 19 vertical levels and a model top at 10 hPa. The ocean model MPIOM [*Jungclaus et al.*, 2006] uses a conformal mapping grid with a horizontal grid spacing of 3.0° and 40 vertical levels.

[7] Volcanic forcing is calculated online, using a time series of AOD at 0.55 μm as well as effective particle radius (R_{eff}), with a fixed standard deviation of 1.8. The data are specified on four equal-area latitude bands with a time resolution of ten days. The eruption start date is set at 1 January 1258 (Figure 1b). AOD estimates [*Crowley et al.*, 2008] are based on a correlation between sulfate in Antarctic ice cores and satellite data [*Sato et al.*, 1993]. R_{eff} growth and decay is also based on satellite observations of Pinatubo [*Sato et al.*, 1993]. Eruptions with AOD larger than 0.2 (maximum AOD of Pinatubo is 0.15) are empirically scaled by comparison with the theoretical calculations for very large eruptions [*Pinto et al.*, 1989]. In the vertical, AOD is divided between 20 and 86 hPa over three model levels, with a maximum at 50 hPa. Sensitivity experiments for the model response to the Pinatubo eruption yield an average global temperature change (0.4 K) comparable to observations.

[8] In order to assess the uncertainties of the climate forcing, we carried out three experiments under the assumption of aerosol mass conservation and constant aerosol lifetime. The first experiment is consistent with *Pinto et al.* [1989] and displays a maximum aerosol effective radius of 0.7 μm after nine months ($R_{0.7}$). In the second experiment we assume that the aerosol size did not increase and remained at the background effective radius of 0.2 μm ($R_{0.2}$). In the third experiment we doubled the increase in aerosol size above background of experiment $R_{0.7}$ reaching a maximum effective radius of 1.3 μm after nine months ($R_{1.3}$). An assumed maximum effective radius of 1.3 μm in experiment $R_{1.3}$ is near the maximum size we obtain in global aerosol simulations for the enormous Yellowstone caldera eruption about 640,000 years ago [*Timmreck et al.*, 2009]. Decreasing the particle radius at a fixed aerosol mass implies a much larger particle number and therefore larger extinction of visible light. We therefore calculate the mass-consistent effect of altered R_{eff} on AOD. Compared to $R_{0.7}$, $R_{0.2}$ yields a much larger, and $R_{1.3}$ a much smaller AOD, respectively (Figure 1b).

[9] An ensemble of ten simulations is carried out for each of the three cases. The simulation period is ten years. All ensemble members are initialized with the same ocean conditions but with infinitesimally different atmospheric horizontal diffusion. To assess the influence of a different initial ocean state, 10 additional ensemble members for $R_{0.7}$ were set up on another ocean state ($R_{0.7O}$). The additional control integration, without volcanic eruptions, was also run with ten ensemble members.

3. Results

[10] Figure 2 shows differences in the net fluxes both at the top of the atmosphere (TOA) and at the surface for the three simulations of the 1258 eruption. Significant flux anomalies are visible for the first year after the eruption. Over time the signal fades away and after about five years the anomaly is not detectable. For the Earth's surface a reduction of incoming solar radiation occurs. This reduction is mainly a function of the AOD. This AOD is largest for $R_{0.2}$ with an averaged annual value of 0.82 and a corresponding surface net flux anomaly of -10.5 W/m^2 in 1258. It is smallest for $R_{1.3}$ with an AOD of 0.24 and a surface flux anomaly of -4.1 W/m^2. It would be even smaller if a higher sedimentation rate for larger particles were considered. At the TOA the volcanic aerosol impacts the radiative energy balance by reflecting solar radiation back to space (albedo effect) and by trapping terrestrial radiation (greenhouse effect). The terrestrial IR effect at the assumed aerosol sizes is driven by absorbing mass. Thus, by conserving aerosol mass and aerosol altitudes for the three simulations, no significant differences in the greenhouse effect are depicted (dotted lines, Figure 2). In contrast, the albedo effect is strongly modulated by the assumed aerosol size. Since the albedo effect dominates, the overall net-

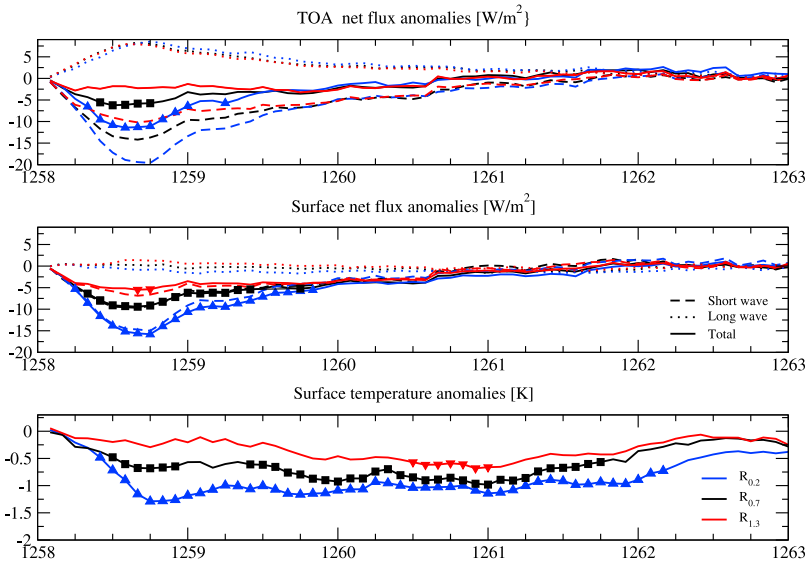

Figure 2. Globally averaged net flux anomalies (top) at the top of the atmosphere (TOA) [W/m^2], (middle) at the surface, and (bottom) near surface temperature anomalies [K]. Black line is original data set ($R_{0.7}$); blue line is same mass as in $R_{0.7}$ but at the constant background effective radius ($R_{0.2}$); and red line is same mass as in $R_{0.7}$ but at a higher effective radius ($R_{1.3}$); see text. Solid symbols indicate monthly mean values that are statistically significant on the 90% confidence level.

effect of volcanic aerosol in all three simulations is a cooling of the Earth-Atmosphere-System.

[11] While the stratospheric warming is similar for all three experiments (see Figure S2), and determined by the stratospheric aerosol load, the strength and temporal development of the tropospheric cooling is clearly a function of aerosol size and modulated by tropical ocean dynamics (Figure 2). Maximum cooling appears delayed with larger aerosol sizes. However, its timing is complicated by an El Niño/La Niña impact especially for responses of experiments $R_{0.7}$ and $R_{1.3}$ (Figure 2). The historical state of the tropical Pacific Ocean during the eruption is extremely difficult to reconstruct. Far-field climate proxies suggest a moderate to strong El Niño event in 1258/1259 [*Emile-Geay et al.*, 2008]. Preliminary analysis of coral data also suggests no clear cooling in 1258 (K. Cobb, personal communication, 2009). Because the ensemble simulations of the 1258 eruption start from an ocean state where an El Niño event was subsiding, there will be inevitable differences between model and data in the tropics. The impact of the 1258 eruption on tropical Pacific Ocean dynamics requires considerably further investigation before any conclusions can be drawn as to verification.

[12] To assess our ESM simulations we compare the simulated near surface temperature anomalies to a new terrestrial temperature reconstruction (Crowley et al., manuscript in preparation, 2009) that is representative of summer half-year (April to September) land temperatures between 30°N and 90°N (Figure 3a). The temperature reconstruction is derived from sites that only have records throughout the past 1000 years (i.e, "no space biasing") and which are fairly evenly distributed. Since the climate model exhibits realistic high inter annual variability (ensemble standard deviation of summer half-year temperatures exceeds 1.5 K), only the largest summer temperature anomalies in the years 1258 and 1259 of $R_{0.7}$, and 1258 to 1260 of $R_{0.2}$, are significant at the 90% confidence level (Figure 3a). Figure 3b also shows a comparison from the Swiss Alps [*Büntgen et al.*, 2006]. In contrast to the hemispheric picture, for Central Europe the best match can be obtained if the eruption is assumed to occur in 1257.

[13] Our comparisons in Figure 3 indicate that the simulated temperature response with respect to effective radii in the range between 0.7 μm and 1.3 μm best matches the terrestrial temperature reconstructions over the Northern Hemisphere following the large volcanic eruption. An additional ensemble of experiments with varied initial ocean conditions, i.e., a more neutral ENSO state (green line), exhibit a temperature response very similar to that of $R_{0.7}$, thereby suggesting that the full ocean variability would not significantly change our conclusion.

4. Discussion and Conclusions

[14] Our study suggests that the cooling effect of a large volcanic eruption is more consistent with recent temperature reconstructions if the aerosol particles are significantly larger than those observed after the 1991 Pinatubo eruption. Several factors could complicate interpretation of our results. Our application of an Antarctic AOD calibration to Greenland may not be valid due to higher precipitation rates (and possibly higher rates of sulfur fallout) over Greenland, although preliminary results argue for it. Sensitivity to volcanic eruptions could also vary with magnitude. However, the sensitivity of volcanic eruptions for the interval 1300–1900 is consistent with sensitivity estimates derived over the instrumental period [*Hegerl et al.*, 2006].

[15] Differences between simulated and estimated temperatures could conceivably result from a systematic bias in tree-rings due to a possible photosynthesis and tree growth enhancement resulting from a shift from direct to diffuse radiation, which leads to a more evenly illuminated canopy [*Robock*, 2005; *Gu et al.*, 2003]. However, global radiation is reduced, which decreases photosynthesis. Our simula-

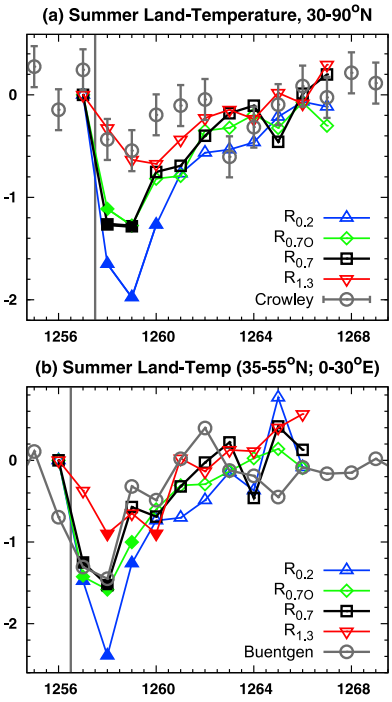

Figure 3. (a) Comparison of a new multi-proxy temperature reconstruction for the growing season over land (grey circles) from 30°N to 90°N (Crowley et al., manuscript in preparation, 2009) and (b) tree-ring data from the Swiss Alps [*Büntgen et al.*, 2006] with simulated near surface temperature anomalies (coloured lines) for the same land areas. Model and temperature reconstructions are averaged values over the summer half year (April–September). The 100 year mean (1157–1256) of the respective data-reconstruction is subtracted. The ensemble standard deviation of the modeled temperature data is 1.5 K for Figure 3a and 1.3 K for Figure 3b. Solid symbols mark statistically significant values above the 90% confidence level. The estimated standard deviation of the proxy data is 0.2 K for Figure 3a. Note that the eruption, indicated by the grey line, is assumed to occur one year earlier in Figure 3b.

tions indicate that the reduction in global radiation is amplified more with increasing AOD than the gain in diffuse radiation (see Table S1). Therefore, we interpret the diffuse enhancement effect to be of limited importance with respect to very large volcanic eruptions.

[16] Microphysical model simulations [*Pinto et al.*, 1989; *Bekki et al.*, 1996] also show that for very large volcanic eruptions, the temporal development of the aerosol size distribution involves many nonlinear processes. Due to a higher gravitational sedimentation rate, larger particles will be removed within a very short time and the aerosol lifetime will be reduced. On the other hand, after very large volcanic eruptions the OH radicals might be depleted and therefore the conversion rate from SO_2 to sulfuric acid vapor reduced [*Bekki*, 1995; *Savarino et al.*, 2003]. This would impede the growth of the aerosol particles and prolong their atmospheric lifetime. Hence, only simulations of the volcanic aerosol size distribution with a fully coupled aerosol chemistry and microphysics model can provide a consistent time-varying data set of aerosol optical parameters. However, simulations of aerosol chemistry interactions with a global ESM over a millennial time scale are very time consuming and therefore currently not feasible. Despite these limitations, the results presented in this study represent a necessary step forward toward a more complete assessment of the climate response to very large volcanic eruptions. The results also have obvious implications to possible overinterpretation of potential effects of extremely large eruptions, such as the Toba Ash, or their ecological impacts, including extinctions.

[17] **Acknowledgments.** This work benefited from stimulating discussions within the MPI-M Super Volcano and Millennium projects. The authors are grateful to Ulrich Schlese and Monika Esch for their help with the model set up and to Ulf Buentgen for providing his tree ring data. C.T. acknowledges support by the German Science Foundation DFG grant TI 344/1-1. Computations were done at the German Climate Computer Center (DKRZ).

References

Ammann, C., F. Joos, D. S. Schimel, B. L. Otto-Bliesner, and R. A. Tomas (2007), Solar influence on climate during the past millennium: Results from transient simulations with the NCAR Climate System Model, *Proc. Natl. Acad. Sci., U. S. A.*, *104*, 3713–3718.

Barberi, F., M. Coltelli, A. Frullani, M. Rosi, and E. Almeida (1995), Chronology and dispersal characteristics of recently (last 5000 years) erupted tephra of Cotopaxi (Ecuador): Implications for long-term eruptive forecasting, *J. Volcanol. Geotherm. Res.*, *69*, 217–235.

Bekki, S. (1995), Oxidation of volcanic SO_2: A sink for stratospheric OH and H_2O, *Geophys. Res. Lett.*, *22*, 913–916.

Bekki, S., J. A. Pyle, W. Zhong, R. Toumi, J. D. Haigh, and D. M. Pyle (1996), The role of microphysical and chemical processes in prolonging the climate forcing of the Toba eruption, *Geophys. Res. Lett.*, *23*, 2669–2672.

Büntgen, U., D. C. Frank, D. Nievergelt, and J. Esper (2006), Summer temperature variations in the European Alps, AD 755–2004, *J. Clim.*, *19*, 5606–5623.

Clausen, H. B., C. U. Hammer, C. S. Hvidberg, D. Dahl-Jensen, J. P. Steffensen, J. Kipfstuhl, and M. R. Legrand (1997), A comparison of the volcanic records over the past 4000 years from the Greenland Ice Core Project and Dye 3 Greenland ice cores, *J. Geophys. Res.*, *102*, 26,707–26,723.

Crowley, T. J. (2000), Causes of climate change over the past 1000 years, *Science*, *289*, 270–277.

Crowley, T. J., G. Zielinski, B. Vinther, R. Udisti, K. Kreutz, J. Cole-Dai, and E. Castellano (2008), Volcanism and the Little Ice Age, *PAGES News*, *16*, 22–23.

Emile-Geay, J., R. Seager, M. A. Cane, E. C. Cook, and G. H. Haug (2008), Volcanoes and ENSO over the past millennium, *J. Clim.*, *21*, 3134–3148, doi:10.1175/2007JCLI1884.

Gao, C., A. Robock, and C. Ammann (2008), Volcanic forcing of climate over the past 1500 years: An improved ice-core-based index for climate models, *J. Geophys. Res.*, *113*, D23111, doi:10.1029/2008JD010239.

Gu, L., D. Baldocchi, S. C. Wofsy, J. W. Munger, J. J. Michalsky, S. P. Urbanski, and T. A. Boden (2003), Response of a deciduous forest to the Mount Pinatubo eruption: Enhanced photosynthesis, *Science*, *299*, 2035–2038.

Hegerl, G. C., T. J. Crowley, W. T. Hyde, and D. J. Frame (2006), Climate sensitivity constrained by temperature reconstructions over the past seven centuries, *Nature*, *440*, 1029–1032.

Hegerl, G. C., et al. (2007), Detection of human influence on a new, validated 1500-year temperature reconstruction, *J. Clim.*, *20*, 650–666.

Jungclaus, J. H., et al. (2006), Ocean circulation and tropical variability in the coupled model ECHAM5/MPI-OM, *J. Clim.*, *19*, 3952–3972.

Langway, C. C., Jr., K. Osada, H. B. Clausen, C. U. Hammer, and H. Shoji (1988), An inter-hemispheric volcanic time-marker in ice cores from Greenland and Antarctica, *Ann. Glaciol.*, *10*, 102–108.

Mann, M. E., et al. (2008), Proxy-based reconstructions of hemispheric and global surface temperature variations over the past two millennia, *Proc. Natl. Acad. Sci., U. S. A.*, *105*, 13,252–13,257, doi:10.1073/pnas.0805721105.

Oppenheimer, C. (2003), Ice core and palaeoclimatic evidence for the timing and nature of the great mid-13th century volcanic eruption, *Int. J. Climatol.*, *23*, 417–426.

Pinto, J. R., R. P. Turco, and O. B. Toon (1989), Self-limiting physical and chemical effects in volcanic eruption clouds, *J. Geophys. Res.*, *94*, 11,165–11,174.

Raddatz, T. J., et al. (2007), Will the tropical land biosphere dominate the climate-carbon cycle feedback during the twenty-first century?, *Clim. Dyn.*, *29*, 565–574.

Robock, A. (2005), Cooling following large volcanic eruptions corrected for the effect of diffuse radiation on tree rings, *Geophys. Res. Lett.*, *32*, L06702, doi:10.1029/2004GL022116.

Roeckner, E., et al. (2006), Sensitivity of simulated climate to horizontal and vertical resolution in the ECHAM5 atmosphere model, *J. Clim.*, *19*, 3771–3791.

Sato, M., J. E. Hansen, M. P. McCormick, and J. B. Pollack (1993), Stratospheric aerosol optical depths, 1850–1990, *J. Geophys. Res.*, *98*, 22,987–22,994.

Savarino, J., S. Bekki, J. Cole-Dai, and M. H. Thiemens (2003), Evidence from sulfate mass independent oxygen isotopic compositions of dramatic changes in atmospheric oxidation following massive volcanic eruptions, *J. Geophys. Res.*, *108*(D21), 4671, doi:10.1029/2003JD003737.

Stothers, R. (2000), Climatic and demographic consequences of the massive volcanic eruption of 1258, *Clim. Change*, *45*, 361–374, doi:10.1023/A:1005523330643.

Taylor, K. C., R. B. Alley, G. W. Lamorey, and P. A. Mayewski (1997), Electrical measurements on the Greenland Ice Sheet Project 2 core, *J. Geophys. Res.*, *102*, 26,511–26,517.

Timmreck, C., S. Lorenz, U. Niemeier, and S. V. Group (2009), The climate impact of a Yellowstone super eruption: An Earth system approach, paper presented at General Assembly 2009, Eur. Geosci. Union, Vienna.

Traufetter, F., H. Oerter, H. Fischer, R. Weller, and H. Miller (2004), Spatio-temporal variability in volcanic sulphate deposition over the past 2 kyr in snow pits and firn cores from Amundsenisen, Antarctica, *J. Glaciol.*, *50*, 137–146.

Wetzel, P., A. Winguth, and E. Maier-Reimer (2005), Sea-to-air CO_2 fluxes from 1948 to 2003, *Global Biogeochem. Cycles*, *19*, GB2005, doi:10.1029/2004GB002339.

T. J. Crowley, School of GeoSciences, University of Edinburgh, Edinburgh EH9 3JW, UK.

J. H. Jungclaus, S. Kinne, S. J. Lorenz, T. J. Raddatz, and C. Timmreck, Max-Planck Institute for Meteorology, Bundesstr. 53, D-20146 Hamburg, Germany. (claudia.timmreck@zmaw.de)

M. A. Thomas, School of Environmental Sciences, University of East Anglia, Norwich NR4 7TJ, UK.